

Investigation of microstructural properties of nitrogen doped ZnO thin films formed by magnetron sputtering on silicon substrate

M. NICOLESCU, M. ANASTASESCU, S. PREDA, J. M. CALDERON-MORENO, P. OSICEANU, M. GARTNER*, V. S. TEODORESCU^a, A. V. MARALOIU^a, V. KAMPYLAFKA^b, E. APERATHITIS^b, M. MODREANU^c

Institute of Physical Chemistry, Romanian Academy, Spl. Independentei 202, 060021 Bucharest, Romania

^aNational Institute of Material Physics, 105 bis Atomistilor Street, 077125 Bucharest – Măgurele, Romania

^bFORTH-IESL, Crete, Greece

^cTyndall National Institute, University College Cork, Cork, Ireland

Zinc oxide (ZnO) is a semiconductor with a wurtzite-type structure, useful for a variety of optical, optoelectronic and piezoelectric applications. We report here on the post deposition treatment (Rapid Thermal Annealing at 400 and 550°C) impact on the microstructural properties of N-doped ZnO (ZnO:N) thin films grown on silicon substrate by r.f. magnetron sputtering of ZnN target. The ZnO:N films have been characterized by X-ray Diffraction (XRD), Atomic Force Microscopy (AFM), Scanning (SEM) and Transmission (TEM) Electron Microscopy coupled with Energy Dispersive X-ray (EDX) and Selected Area Electron Diffraction (SAED) respectively and Fourier Transform Infrared (FTIR) Spectroscopy. XRD confirms that ZnO:N films are polycrystalline in the as deposited state. SEM, TEM and XRD measurements revealed a polycrystalline film with preferentially oriented columnar crystals. AFM studies reveal a drastic change of ZnO surface morphology upon RTA and the existence of areas with different roughness in the sample thermally treated at 400°C. FTIR, XRD and TEM results shows that disorder associated mainly with grain boundary defects decreases as the annealing temperature increases.

(Received March 31, 2010; accepted May 26, 2010)

Keywords: N-doped ZnO, Magnetron sputtering, AFM, XRD, SEM & EDX, XPS, TEM & SAED, FTIR

1. Introduction

ZnO possesses the same wurtzite-type structure (group-III nitrides) as GaN, and thus belongs to the space group C_6^4 v. ZnO is a direct-band-gap material ($E_g \approx 3.37$ eV) with large exciton binding energy $E_{ex} \approx 60$ meV [1], this makes it feasible for optoelectronic devices [2] light-emitting devices [3], gas sensor [4], solar cells [5], transistor [6] and photocatalysts operating in the UV range. All the ZnO films proved excellent UV shielding due to the absorption edge on the short wavelength side ($\lambda \sim 300$ nm). Apart from this, high reflectance in the IR region can make this film a good candidate for application as the coating for heat reflectors, as well as in other fields of technology. All these applications require a good uniformity of films and high electrical conductivity simultaneously with high optical transmission in the visible region.

Many techniques have been employed in the deposition of thin films ZnO such as sol gel [7,8], layer-by-layer [9], chemical vapour deposition [10], sputtering [11] and so on, using as starting material Zn or ZnO.

We report here on the fabrication of ZnO films on monocrystalline silicon by r.f. sputtering from ZnN target and on the impact of Rapid Thermal Annealing (RTA) on the microstructural properties of the films. These

properties and their evolution following RTA have been investigated by X-ray diffraction (XRD), Atomic Force Microscopy (AFM), scanning (SEM) and transmission (TEM) electron microscopy coupled with Energy Dispersive X-ray (EDX) and Selected Area Electron Diffraction (SAED) respectively and Fourier Transform Infrared (FTIR) spectroscopy.

2. Experimental

2.1 Film preparation

Nitrogen doped ZnO (ZnO:N) thin films were deposited by rf magnetron sputtering using ZnN target (99.9% purity) on, unintentionally heated, Si substrates. The substrates were ultrasonically cleaned in acetone and isopropanol, rinsed in deionizer water and dried in flowing nitrogen gas. The native oxide on Si surface was etched in HF solution before the substrates were introduced into the sputtering system. Prior to deposition, the target was pre-sputtered for at least 15min (Ar plasma, 5mTorr, 100W rf-power) to remove any contaminants from the target surface and to enable equilibrium conditions to be reached. The rf-power was kept at 100W the ratio of gases flow rates was Ar:O₂:N₂=5:4:1 and the total pressure was 5mTorr. Following deposition, the ZnO samples were

treated by Rapid Thermal Annealing (RTA) for 1 min in N₂ atmosphere, at 400 and 550°C.

2.2. Characterization methods

The crystallinity of the as prepared and thermally treated ZnO:N films was studied by X-ray diffraction (XRD) method. The measurements were performed using Rigaku Ultima IV equipment, with Cu K α radiation and a fixed power source (40 kV and 30 mA). The diffractometer was set in condition of grazing incident X-ray diffraction (GIXD) with $\omega = 0.5^\circ$. The films were scanned at a rate of $5^\circ (2\theta)/\text{min}$ over a range of $5\text{--}90^\circ$.

Atomic force microscopy (AFM) measurements were performed in order to examine the surface morphology. EasyScan2 model from Nanosurf® AG Switzerland instrument was employed with a high resolution scanner of $10\ \mu\text{m} \times 10\ \mu\text{m} \times 2\ \mu\text{m}$ working in the intermittent-contact and contact modes and by using sharp tips (radius of curvature of less than 10 nm) from Nanosensors™.

Scanning Electron Microscopy (SEM) was used to examine the surface morphology, at a bigger scale than AFM, using a Jeol JSM-840 microscope equipped with an INCA Energy 250 (Oxford Instruments) energy dispersive X-ray (EDX) system and a Zeiss EVO LS10 environmental SEM microscope.

The conventional TEM images and the SAED patterns were recorded using a Jeol 200CX electron microscope and the high resolution images on a Topcon 002B electron microscope. Specimens for TEM observations were prepared by the cross section method. The EDX measurement were performed on the XTEM specimens and on specimens mechanically extracted from the film [12].

Surface analysis performed by X-Ray Photoelectron Spectroscopy (XPS) was carried out on VG K-Alpha equipment, with a base pressure in the analysis chamber of 10^{-9} Torr. The X-ray source was AlK α radiation (1486.6eV, monochromatized) and the overall energy resolution is estimated at 0.5 eV by the full width at half maximum (FWHM) of the Au4f_{7/2} line. After (0-1100 eV) survey scans, high resolution scans over narrow energy ranges were recorded around each peak of interest. In order to take into account the charging effect on the measured Binding Energies (BE's) the spectra were calibrated using the C1s line (BE = 285.0 eV) of the adsorbed hydrocarbon on the sample surface and the flood gun was used during recording spectra.

Fourier Transform Infrared (FTIR) Spectroscopy transmission measurements have been performed in far IR at normal incidence using a Varian FTS7000 system equipped with a Peltier cooled DTGS detector. The resolution was 4cm^{-1} and 100 scans have been co-added. A bare substrate has been used as reference for the measurements.

3. Results and discussion

3.1 XRD

All samples presented only the peaks of ZnO from: (002), (101), (103) and (102) according to JCPDS data card 36-1451. The fresh film is full crystallized as evidenced XRD in the Fig. 1. With the thermal treatment (TT) the bands are narrower and their intensity become higher thus means the quality of the crystalline phase increases. The position of the peak (002) has been compared with literature assignment as seen in Table1.

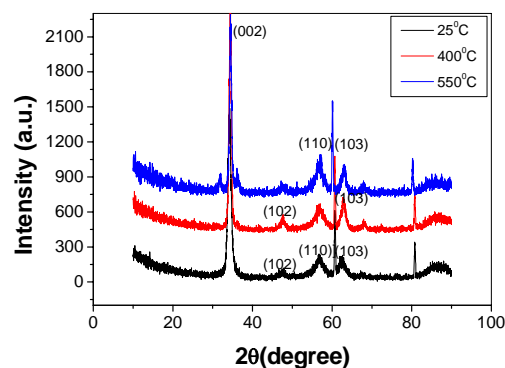


Fig. 1. XRD spectra of as-deposited and RTA (400 and 550°C) ZnO:N films deposited on silicon.

The peak located at $2\theta = 34.25^\circ$ indicates that the (002) orientation dominates in films deposited on Si, proving the existence of a ZnO single-phase with a hexagonal wurtzite structure. The crystalline grain size increases upon RTA annealing while the FWHM of diffraction peak decreases. These results have shown that an improvement of the crystalline state is obtained following RTA annealing.

Table 1. Crystalline grain size and position of the main diffraction peak for as-deposited and RTA (400 and 550°C) ZnO:N films.

Sample	(hkl)	2 θ (degree)	FWHM (degree)	Crystallite size (nm)
25°C	(002)	34.25	0.96	9.02 \pm 0.1
400°C	(002)	34.48	0.68	12.70 \pm 0.1
550°C	(002)	34.43	0.69	12.55 \pm 0.1

* FWHM- full width at half maximum

3.2. AFM

The topography of the ZnO films was found to be dependent on the substrate used for deposition in terms of morphological features and roughness as well. In Fig. 2a it could be seen the surface of the ZnO:N film freshly deposited on Silicon (untreated) revealing elongated surface particles (with dimensions on the longest axis around 400 nm) and a much higher RMS roughness as compared with glass substrate (images not shown): 21 nm for silicon vs. 2 nm on glass at a scale of $2 \times 2\ \mu\text{m}^2$. Due to

the presence of these large particles (elongated shape), the surface of the untreated films deposited on Silicon exhibits a high roughness, around 22-25 nm – almost independent on scale of measurements.

On the surface of the film treated at 400°C there are different areas with different roughness at larger scales (scanned areas of $8 \times 8 \mu\text{m}^2$) from few nm up to tens of nm. The areas having different roughness could be correlated with their different colours as follows: the lowest roughness (with formation of rounded small grains) was seen on yellow parcels while an abrupt increase in roughness was observed by moving to magenta coloured parcels. This high roughness originates in the protruding large particles (columnar grown), generally rounded shaped (rectangular particles were also observed) with a diameter around 100-200 nm. On smooth (yellow) areas, small grains (20-30 nm mean diameter) could be seen in Fig. 2b – giving a local RMS roughness of around 4 nm.

Increasing the temperature of thermal treatment to 550°C (Fig. 2c) the smooth (yellow) areas are no more visible, but rough (magenta-like). On small areas, the formation of compacted grains could be noticed (with a diameter a bit larger, around 60-80 nm and even larger). If comparing with the superficial grains in the sample treated at 400°C, it may be possible that the superficial particles (grains) become bigger after thermal treatment at 550°C due to effect of coalescence. The morphological features observed for both thermally treated films (at 400 and 550°C) at larger scales are in agreement with SEM images, shown in the next paragraph. However, the most important morphologic aspect seen by AFM on the ZnO:N films deposited on Silicon is the textural isotropy of the thermally treated samples (with round particles on the surface) in contrast with the untreated sample.

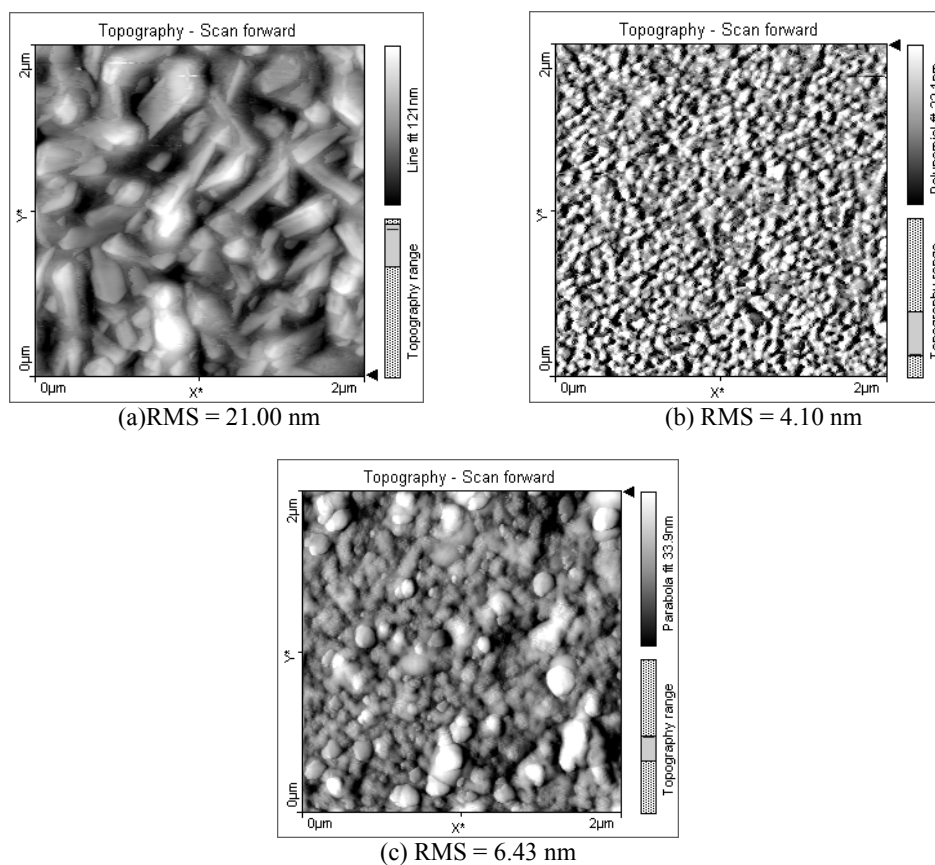


Fig. 2. Topographic images at a scale of $2 \times 2 \mu\text{m}^2$, presenting the morphology of the ZnO:N films deposited on Silicon: (a) as deposited, (b) after RTA at 400°C and (c) after RTA at 550°C

3.3. SEM

SEM observations demonstrated a complete coating of the substrates. Fig. 3 shows the morphology of the coatings of ZnO:N before and after thermal treatments at 400 and 550°C, respectively. The observed morphology after deposition corresponds to dense polycrystalline films,

evidenced by protruding nanocrystallites, sized up to around 100 nm diameter, and homogeneously distributed over the whole coating surface, in as deposited and thermally treated samples. The coatings are fully dense, without open porosity, making a compact two-dimensional layer, with protruding grains that indicate the growth of single-crystal columnar ZnO structures. From this

structure we only see the tip. ZnO is a polar crystal and its polar axis is the *c*-axis, leading to anisotropic growth of *c*-axis oriented ZnO one-dimensional crystals [13]. The preferential orientation of the ZnO film in the (002) direction, consistent with the growth of *c*-axis oriented ZnO rods, is confirmed by the XRD pattern (above) and TEM measurements (below).

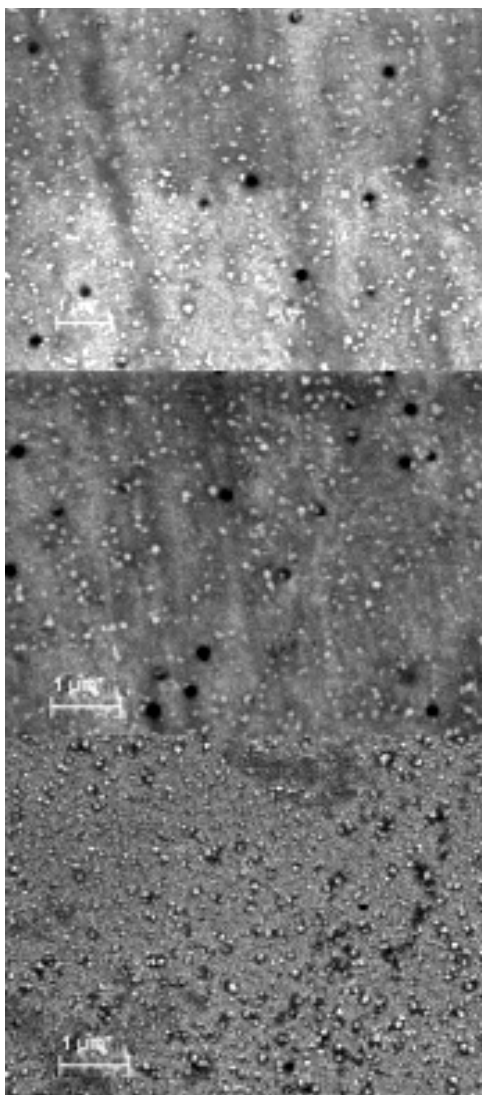


Fig. 3. SEM micrographs of (a) the as-deposited ZnO:N film; (b) ZnO:N film after RTA at 400°C; (c) ZnO:N film after RTA at 550°C.

3.4 XPS

The XPS results reveal that the O1s line (not shown here) is gradually shifted towards the O²⁻ (ZnO) Binding Energy (BE) with the increasing RTA temperature. The XPS showed the presence of nitrogen in the RTA ZnO:N samples (see Fig. 4a). The band-like shapes of the Auger Zn-L₃M₄₅M₄₅ spectra (Fig. 4b) for as-deposited and RTA ZnO:N thin films suggests a mixture of Zn oxide and hydroxide buried under a rather thick carbon layer.

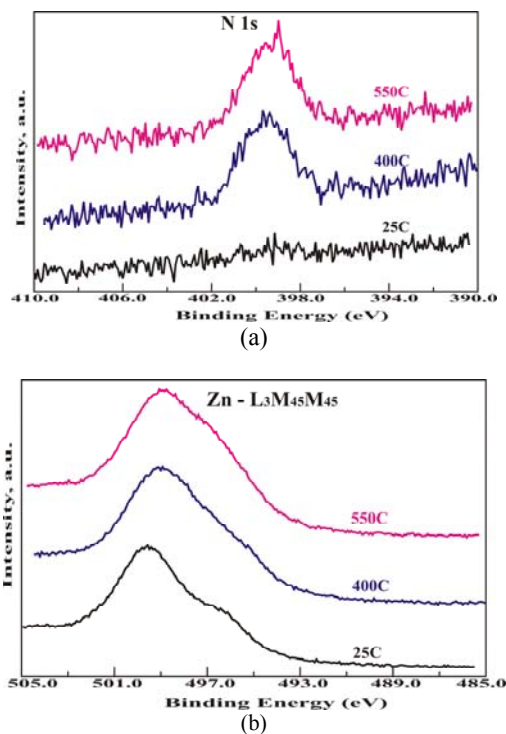


Fig. 4. (a) The N1s proportional superimposed photoelectron spectra showing the presence of trace amounts of nitrogen on the surfaces of the annealed samples (RTA at 400 and 550°C); (b) Auger Zn-L₃M₄₅M₄₅ spectra in ZnO:N films

The quantification of the XPS results for as-deposited and RTA ZnO:N thin films is shown in Tables 2-4. For the as-deposited ZnO:N thin film (Table 2) we notice that the oxygen is, apparently, found in excess related to the ZnO stoichiometry. However we detect the presence of water, OH adsorbed groups and OH-C-O, O=C chemical bondings as well. For the ZnO:N sample, RTA at 400°C (see Table 3) the appearance of N 1s with two components which are assigned to zinc nitride (lower BE) and diluted zinc oxynitride (higher BE). Obviously, the same statement as above can be made on the oxygen excess. Increasing the RTA annealing temperature to 550°C, we notice that the amount of nitrogen slightly increases and only O-C and O=C can be detected besides zinc oxide and zinc oxynitride (see Table 4).

Table 2. XPS quantification of the as-deposited ZnO:N sample from narrow region spectra

Elements	O	Zn	N
Photoelectron lines	1s	2p _{3/2}	1s
Binding Energies(eV)	530.9, 532.1	1022.3	-
Relative concentrations (atom %)	59.8	40.2	-

Table 3. XPS quantification of the RTA (400°C) ZnO:N sample from narrow region spectra

Elements	O	Zn	N
Photoelectron lines	1s	2p3/2	1s
Binding Energies(eV)	530.7, 532.1	1022.1	398.8, 400.2
Relative concentrations (atom %)	56.3	42.5	1.2

Table 4. XPS quantification of the RTA (550°C) ZnO:N sample from narrow region spectra

Elements	O	Zn	N
Photoelectron lines	1s	2p3/2	1s
Binding Energies(eV)	530.9, 532.3	1022.2	398.7, 400.1
Relative concentrations (atom %)	52.6	45.5	1.9

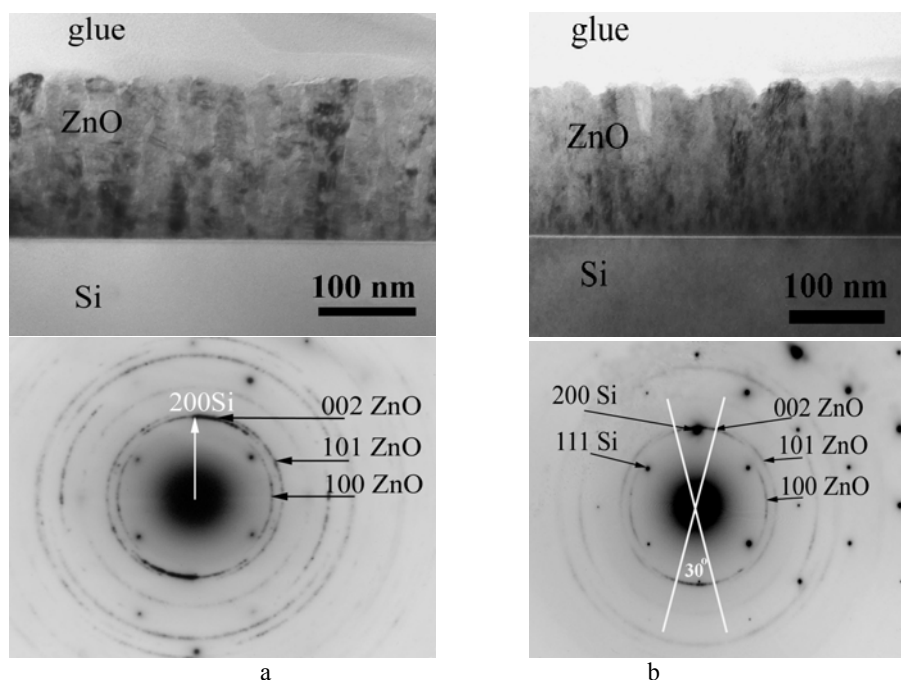


Fig. 5. TEM & SAED images of: (a) as-deposited ZnO:N film; (b) ZnO:N film RTA at 400°C.

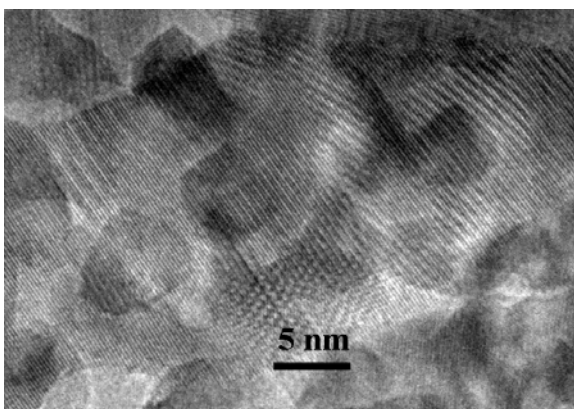
3.5 TEM & SAED

In Fig. 5 are presented the XTEM and the corresponding SAED images of the ZnO films, before and after annealing at 400°C. Both SAED patterns contain spots from the ZnO thin film and from the Si substrate, which is close to the $\langle 110 \rangle$ orientation. The film thickness is around 170 nm. The SAED patterns clearly indicate the $\langle 001 \rangle$ orientation of the columnar morphology if the ZnO films.

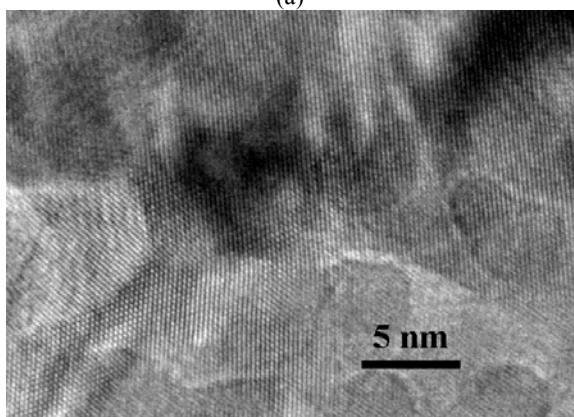
As the SAED patterns are taken in XTEM configuration, the direction perpendicular on the ZnO:N film surface shows the (100) and (101) reflections.

The (002) reflection appears only in the direction parallel to the film surface. The spread of the $\langle 001 \rangle$ directions is about 30° as can be seen the SAED patterns.

In low magnification images, the columnar structure of the film is similar before and after annealing. The columnar morphology contrast indicates a much defected structure inside the columnar grains. The columnar grain diameter varies from about 10 nm at the bottom part of the film to about 50 nm at the surface. The average size of the coherent crystal blocks is between 10 and 20 nm, as revealed by the Bragg contrast variation inside the columnar grains. Some differences can be seen in the high resolution images exposed in Fig. 6.



(a)



(b)

Fig. 6. HRTEM images of the bottom part of the ZnO:N film imaged in the XTEM specimens: (a) before annealing and (b) after annealing at 400°C

As can be observed in the high resolution images taken at the bottom part of the film, the coherence of the ZnO lattice directions is stronger than the limits of the morphological film grains. These limits can be limits of some nanopores in the film. At this part of the film, the $\langle 001 \rangle$ texture is only incipient, the possible nanopores are surrounded by crystal blocks with the same crystalline orientation, resulted from the film growth process. This aspect was not found for pure ZnO films grown by the same method and can be a sign of the N film doping during growth. The high resolution images show also a larger crystalline coherence after annealing. Fig. 7 shows an EDX spectrum detail collected on a fragment of the ZnO film before annealing. The nitrogen is present with a small peak between the carbon (from the TEM grid) and the oxygen. In the as-deposited film N was not observed in the first monolayers from the surface (from XPS analysis) but as seen in Fig. 7 was detected in the small quantity in the volume of the films. The ratio between the N:O is about 1:6 as the EDX quantitative analysis show. The EDX spectrum is similar for the annealed films, meaning that the nitrogen is not lost during annealing and its concentration is similar for all films.

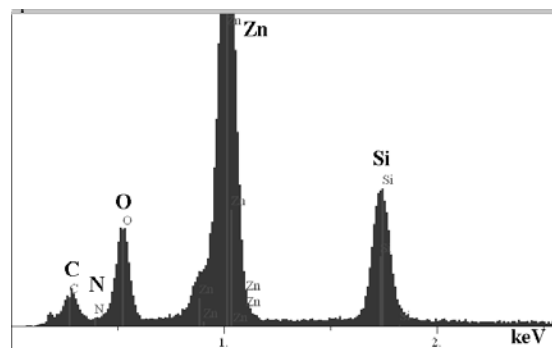


Fig. 7. EDX spectrum of the ZnO:N film before annealing, showing the presence of nitrogen.

3.6. FTIR Spectroscopy

The absorption IR spectra for the as deposited and RTA ZnO:N thin films are shown in the Fig. 8.

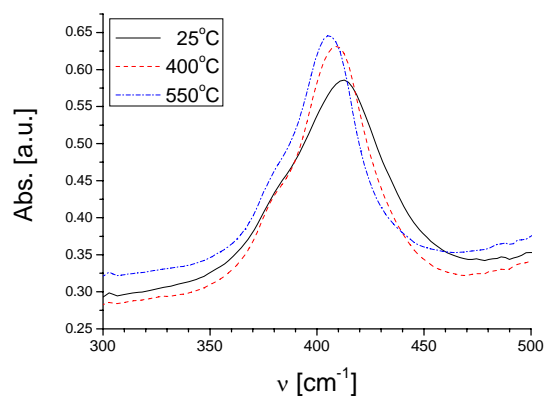


Fig. 8. FTIR absorption spectra of as-deposited and RTA (400 and 550°C) ZnO:N thin films.

The presence of the $E_1(\text{TO})$ phonon peak around 410 cm^{-1} in all spectra indicates that all ZnO:N films are in a crystalline state. It was evidenced that the $E_1(\text{TO})$ broad band for fresh sample narrows and shifts to small wave numbers with the increasing of the temperature of RTA, which indicate the evolution toward a better crystallized structure in agreement with XRD and TEM results.

4. Conclusions

ZnO:N crystalline films were deposited onto silicon substrate by the r.f. sputtering method from ZnN target. The HRTEM reveal a two-layer structure. The growth of ZnO:N film starts with a 20 nm-thick layer that consists of random orientated nanocrystals and followed by a thicker layer of single layer textured (002) columnar layer. The AFM reveals that while the surface of the as-deposited ZnO:N films is rather rough a significant improvement of surface morphology is achieved after RTA treatment. SEM

measurements revealed a polycrystalline film with preferentially oriented columnar crystals and this was found to be in agreement with TEM, electron diffraction and XRD observations.

Nitrogen was detected in small quantity by EDX in the volume of the films, where the ratio between the N:O is about 1:6 in as-deposited film and did not change during annealing. The degree of disorder observed in the as-deposited ZnO:N is significantly reduced after RTA treatment.

Acknowledgement

This work was supported by the Irish SFI Strategic Research Cluster "FORME", Award number 07/SRC/I1172 and partially supported by the Romanian PN2 project number 11061/2007.

References

- [1] G. E. Jellison, L. A. Boatner, *Phys. Rev. B* **58**, 3586 (1998).
- [2] D. P. Norton, Y. W. Heo, M. P. Ivill, et al. *Mater. Today* **7**, 34 (2004).
- [3] M. H. Huang, S. Mao, H. Feick, H. Yan, Y. Wu, H. Kind, E. Weber, R. Russo, P. Yang, *Science* **292**, 1897 (2001).
- [4] H. Xu, X. Liu, D. Cui, M. Li, M. Jiang, *Sensors and Actuators B: Chemical* **114**, 301 (2006).
- [5] J. B. Baxter, E. S. Aydie, *Solar Energy Materials and Solar Cells* **90**, 607 (2006).
- [6] E. M. C. Fortunato, P. M. C. Barquinha, A. C. M. B. G. Pimentel, et al. *Adv. Mater* **17**, 590 (2005).
- [7] M. Miyanchy, A. Nakajima, T. Watanabe, K. Hashimoto, *Chem. Mater.* **14**, 2812 (2002).
- [8] Y. S. Kim, W. P. Tai, S.J. Shu, *Thin Solid Films* **491**, 153 (2005).
- [9] D. Sebok, T. Szabo, I. Dekany, *Appl. Surf. Science* **255**, 6953-6962 (2009).
- [10] S. T. Tan, B. J. Chen, X. W. Sun, X. Hu, X. H. Zhang, S. J. Chua, *J. of Crystal Growth* **281**, 571 (2005).
- [11] R. Das, S. Ray, *J. Phys. D: Appl. Phys.* **36**, 152-155 (2003).
- [12] V. S. Teodorescu, M.G. Blanchin, *Microscopy and Microanalysis* **15**, 15 (2009).
- [13] Z. Wang, X.-F. Qian, J. Yin, Z.-K. Zhu: *J. Solid State Chem.* **177**, 2144 (2004).

*Corresponding author: mgartner@icf.ro